A Nanophotonic Structure Containing Living Photosynthetic Bacteria

*David Coles, Lucas C. Flatten, Thomas Sydney, Emily Hounslow, Semion K. Saikin, Alán Aspuru-Guzik, Vlatko Vedral, Joseph Kuo-Hsiang Tang, Robert A. Taylor, Jason M. Smith, and David G. Lidzey**

***P**hotosynthetic organisms rely on a series of self-assembled nanostructures with tuned electronic energy levels in order to transport energy from where it is collected by photon absorption, to reaction centers where the energy is used to drive chemical reactions. In the photosynthetic bacteria Chlorobaculum tepidum, a member of the green sulfur bacteria family, light is absorbed by large antenna complexes called chlorosomes to create an exciton. The exciton is transferred to a protein baseplate attached to the chlorosome, before migrating through the Fenna–Matthews–Olson complex to the reaction center. Here, it is shown that by placing living Chlorobaculum tepidum bacteria within a photonic microcavity, the strong exciton–photon coupling regime between a confined cavity mode and exciton states of the chlorosome can be accessed, whereby a coherent exchange of energy between the bacteria and cavity mode results in the formation of polariton states. The polaritons have energy distinct from that of the exciton which can be tuned by modifying the energy of the optical modes of the microcavity. It is believed that this is the first demonstration of the modification of energy levels within living biological systems using a photonic structure.*

Dr. D. Coles, Prof. D. G. Lidzey
Department of Physics and Astronomy
University of Sheffield
Sheffield S3 7RH, UK
E-mail: d.g.lidzey@sheffield.ac.uk

L. C. Flatten, Prof. J. M. Smith
Department of Materials
University of Oxford
Sheffield OX1 3PH, UK

Dr. T. Sydney
Department of Chemistry
University of Sheffield
Sheffield S3 7HF, UK

Dr. E. Hounslow
Department of Chemical and Biological Engineering
University of Sheffield
Sheffield S1 3JD, UK

Dr. S. K. Saikin, Prof. A. Aspuru-Guzik
Department of Chemistry and Chemical Biology
Harvard University
Cambridge, MA 02138, USA

Dr. S. K. Saikin
Institute of Physics
Kazan Federal University
Kazan 420008, Russian Federation

Prof. V. Vedral, Prof. R. A. Taylor
Department of Physics
University of Oxford
Oxford OX1 3PU, UK

Dr. J. K.-H. Tang[+]
Department of Chemistry and Biochemistry
Clark University
Worcester, MA 01610-1477, USA

[+]Present address: Materials and Manufacturing Directories, Air Force Research Laboratory, WPAFB, OH 45433, USA

DOI: 10.1002/smll.201701777

Almost all biological organisms interact with light in one form of another. The most obvious manifestation of this is vision, whereby light is absorbed by pigments within the retina and then transducted into an electrical stimulus.[1] It is arguable however that the most important interaction process that occurs in nature is that of photosynthesis.[2] This process is used by both plants and bacteria and ultimately provides the energy to directly or indirectly support most life on Earth. Many biological organisms also use light to communicate. This interaction can occur via a number of mechanisms, including the direct emission of light (bioluminescence[3]), the incoherent scattering of light by dyes and pigments,[4] and through the use of photonic structures to control the reflection and scattering of light to create iridescent structures.[5] This process is used by certain species of birds,[6] beetles,[7,8] and plants,[9] where self-organized micro- and nanostructured layers are used to generate constructive and destructive interference effects.[10]

Instead of simply exploring the optical properties of natural systems, it is interesting to consider whether we can use "top-down" photonic engineering to perturb or modify the function of a biological system. This can both be used to better understand the intricate mechanisms designed by nature to control its interaction with light or perhaps emulate the structures found in nature to create new types of synthetic paints or pigments.[11] We note that there are numerous accounts of the use of photonic crystals for the sensing of biomolecules.[12,13] Recent work has also involved living cells tagged with fluorescent polymer beads that undergo lasing, allowing refractive index changes within the cell to be followed,[14] and inserting a photonic nanobeam probe into living cells to probe their optical properties.[15] Other researchers have modified living cells to express a fluorescent protein, and have placed such cells within an optical cavity to generate lasing.[16] Despite such progress, optical engineering has so far had a relatively minor effect on the electronic energy levels within such organisms. In this Communication, we use optical engineering to modify the energy landscape within living green sulfur bacteria (GSB). To do this, we place the bacteria into an optical cavity and utilize optical strong coupling to modify the energy level of the chlorophyll aggregates within the bacteria that are used by the bacteria to harvest light for photosynthesis. This approach opens an opportunity to deeply understand the interplay of the electronic states within a photosynthetic organism with its biological function. Looking further ahead, we expect that our approach will allow the electronic states within photosynthetic bacteria to be optically hybridized with other optoelectronic materials and will permit us to design bacterial systems that can absorb or emit light by coupling to entirely synthetic external "antennas." This exciting possibility could result in new methods that allow for noninvasive control of photosynthetic processes in vivo.

To modify the electronic energy levels of the light harvesting apparatus of living bacteria, we have placed the bacteria within a microcavity that operates in the so-called "strong-coupling regime." The strong-coupling regime can be accessed when a material having a dipole-allowed transition is placed into a photonic structure that supports a quantized optical mode. If the optical transition of the material is resonant with the energy of the photonic mode, energy can be reversibly exchanged between the cavity mode and the exciton states, with new eigenstates formed that are a coherent superposition of photonic and excitonic transitions. Such states are called cavity polaritons and are quasiparticles that are delocalized throughout the resonator due to their photonic component, while retaining an interaction cross section inherited from the exciton.[17] The mixed light–matter properties of polaritons have led to striking displays of phenomena such as polariton superfluids,[18] inversionless lasing,[19] and nonequilibrium Bose–Einstein condensates,[20] the latter two being observed up to room temperature.[21–23] Strong exciton–photon coupling in optical microcavities was first observed almost 25 years ago by Weisbuch et al.,[24] when a series of semiconductor quantum wells were embedded between two high-quality planar dielectric mirrors. Since then, a variety of materials have been shown to be able to strongly couple to photonic modes such as bulk semiconductors,[25] organic molecules,[26,27] polymers,[28] 2D transition metal dichalcogenides,[29,30] and proteins.[31,32] Recent work has used an array of plasmonic nanostructures to modify the excitonic energy of a photosynthetic complex.[33] We have previously fabricated strong-coupled microcavity structures containing an isolated chlorosome assembly derived from green sulfur bacteria.[34] In such previous work however, the molecular assemblies that were strongly coupled were isolated from their parent organisms. We believe the work presented here makes a significant advance on such previous studies as we strongly couple to aggregate states within functioning bacteria. We believe this is the first observation of the use of photonic engineering to directly modify the electronic energy states within a living organism.

Figure 1a shows a transmission electron microscopy (TEM) image of *Chlorobaculum tepidum* (*Cba. tepidum*). The bacteria were either grown following the procedure given in ref. [36] or purchased as an active culture (Leibniz-Institut DSMZ) and were stored in anaerobic conditions prior to use. Each bacterial cell contains 200–250 light harvesting chlorosomes, which are large ovoid structures (100–200 nm long, ≈50 nm wide) consisting of tubular or planar aggregates of bacteriochlorophyll *c* (BChl *c*) molecules.[37,38] The absorption spectrum of *Cba. tepidum* in aqueous solution (40 mg biomass mL^{-1}) is shown in Figure 1b (green line). The strong absorption peak at 750 nm is due to aggregates of BChl *c* in the chlorosomes. The weak absorption shoulder at 676 nm is assigned to BChl *c* monomer and/or chlorophyll *a* that can be found in the reaction center (while the principle exciton energy of the reaction center is at 840 nm). The shoulder at 810 nm is due to the Fenna–Matthews–Olson (FMO) complex, while the absorption band in the 400–500 nm region is from the Soret band of BChl *c* and carotenoid molecules within the chlorosomes. In order to verify the bacteria are alive in the strong coupling regime, we use the cell viability stain trypan blue (TB, 0.4% in water) which was added to the bacteria solution at a volume ratio of 1:1 and mixed before being injected into the cavity region. The dye is able to permeate the cell membrane of dead cells and binds to intracellular proteins. Live cells with intact membranes are unstained by the dye.[39] The absorption spectrum of TB is shown in Figure 1b (blue line), and displays a strong absorption peak at 587 nm, with a shoulder at 630 nm.

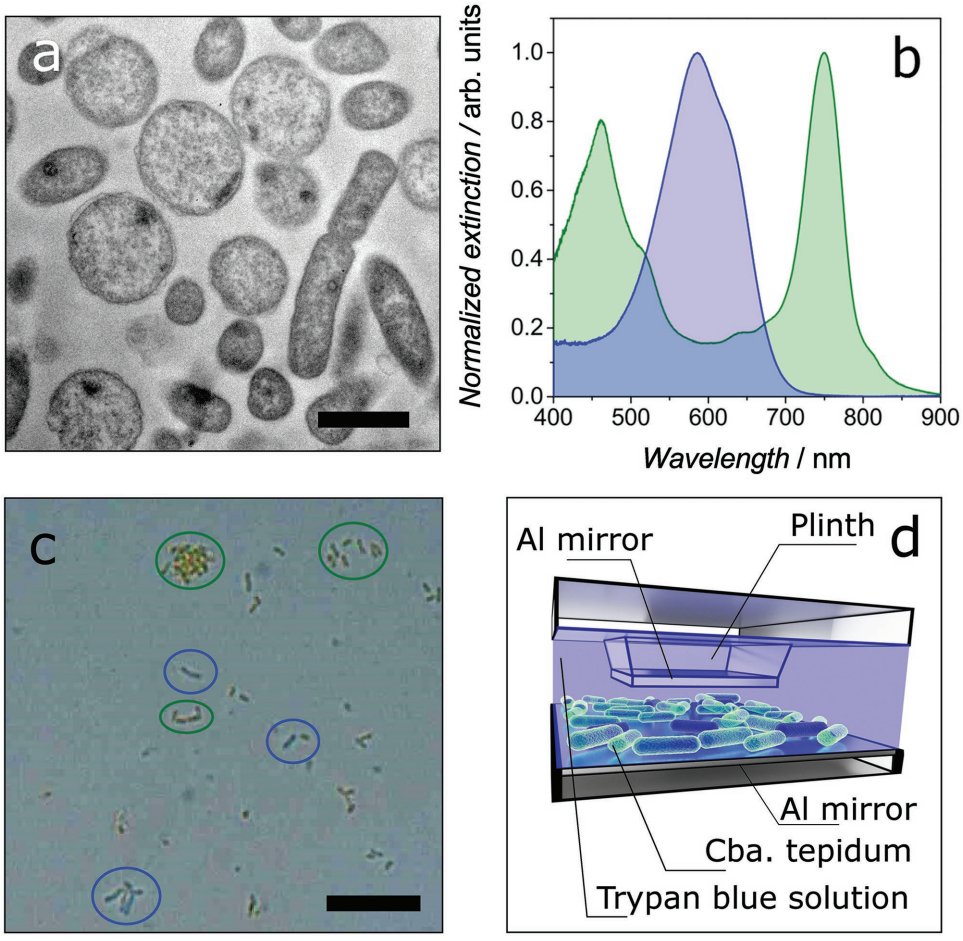

Figure 1. a) TEM image of *Chlorobaculum tepidum (Cba. Tepidum)*. Scale bar is 1 µm. Note that the size and shape of the bacteria is dependent upon the light conditions during growth.[35] b) Normalized extinction spectra of 0.4% trypan blue (TB) aqueous solution (blue line) and *Cba. tepidum* in water (green line). c) Optical microscope image of *Cba. tepidum* in a TB viability stain showing bacteria with compromised cell membranes (stained blue, circled blue) and intact cell membranes (unstained, appear green, circled green). The scale bar is 10 µm. d) Schematic of microcavity consisting of a bacterial solution suspended between two semitransparent metallic mirrors, one of which is on a raised plinth.

Figure 1c shows an optical microscope image of the *Cba. tepidum* solution stained with TB. Both dead and alive bacteria are visible, circled blue and green, respectively.

The microcavity was formed from two 15 nm thick semitransparent aluminum planar mirrors (80% reflectivity at 750 nm) thermally deposited on silica substrates. One of the substrates has a raised "plinth" of dimensions 100 µm × 100 µm onto which the mirror is grown. A 10 nm layer of poly(methyl methacrylate) (PMMA) is spin-cast onto each mirror. The two mirrors are mounted face-to-face to form the cavity within a custom-built white-light transmission microscope that allows angular alignment of the mirrors. A piezoelectric actuator allowed nanometric control over the cavity length. The cavity was imaged onto the entrance slit of an imaging CCD spectrometer. The area to be spectrally imaged was defined by the image position on the spectrometer slit and the row of pixels on the CCD, the former defining the horizontal coordinate and the latter the vertical coordinate.

The cavity mirrors were first aligned to be parallel by observing the interference fringes in transmission as the cavity length was reduced, and adjusting the angle of one of the mirrors until only one fringe is visible across the plinth. The cavity length was scanned by applying a linear voltage ramp to a piezoelectric actuator attached to one of the cavity mirrors, and the cavity transmission was spectrally imaged as a function of time.

The transmission spectra from a region of the cavity measuring 5.5 µm × 1.2 µm as the cavity length is scanned from 450 to 725 nm is shown in **Figure 2**a. The observed transmission peak corresponds to the $q = 2$ cavity mode, where q is the mode index (see the Experimental Section). As the cavity mode energy is scanned through the exciton energy (solid white line), two peaks are observed that anticross about that energy. These peaks are the upper and lower polariton branches (UPB and LPB, red circles) that reside at higher and lower energy than the exciton respectively, and the magnitude of the energy splitting where the uncoupled cavity mode and exciton would be degenerate is the Rabi splitting energy—a measure of the coupling strength of the system. While a strongly coupled system may be described using a fully quantum or semiquantum formalism,[40] here the large number of exciton states within the cavity allow us to use a classically coupled oscillator model[41] to fit the polariton state energies.

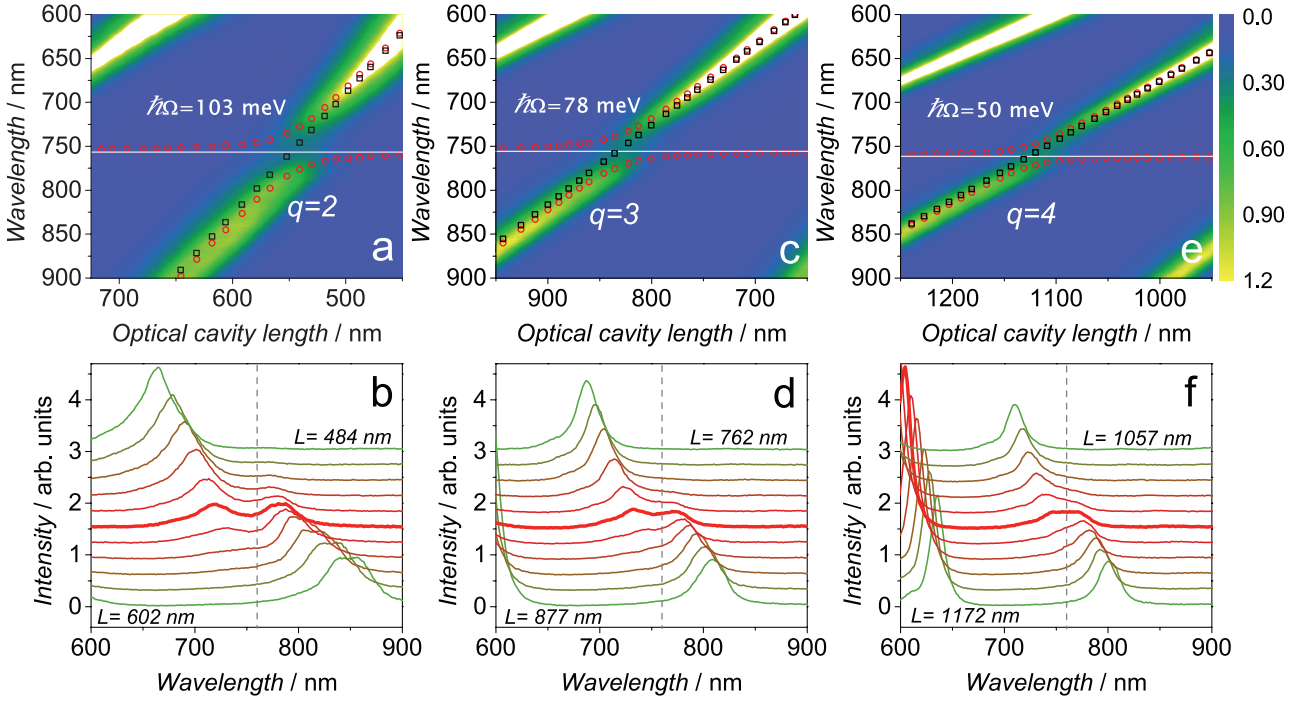

Figure 2. a) Transmission of the cavity at the point labeled **1** in Figure 3 as function of wavelength and cavity length while scanning the $q = 2$ cavity mode through the chlorosome exciton energy, showing the anticrossing of the polariton branches about the chlorosome exciton. White horizontal line shows the chlorosome exciton energy and black squares show the unperturbed cavity mode energy. Red circles are the fitted polariton branch energies. b) Individual transmission spectra, vertically offset, for given cavity lengths around exciton–photon resonance clearly showing the splitting of the cavity mode at exciton–photon resonance. Gray dashed line shows the chlorosome exciton energy. Cavity modes for c,d) $q = 3$ and e,f) $q = 4$, respectively.

The energy of the lower and upper polariton branches is given by a coupled oscillator model.[42] This is fitted to the observed polariton branch energies with the Rabi splitting energy $\hbar\Omega$ and intracavity refractive index n as fitting parameters (see the Experimental Section). In the case of coupling with the $q = 2$ cavity mode, we find a splitting of 103 meV. The criteria for strong coupling[43] is that $\hbar\Omega > (\gamma_x/2) + (\gamma_c/2)$ where γ_x and γ_c are the full-width at half-maximum linewidths of the uncoupled exciton and photon, respectively. The chlorosome exciton linewidth is 130 meV, and the $q = 2$ cavity mode linewidth away from the strong coupling region is 70 meV, therefore the strong coupling criteria is satisfied for coupling to the $q = 2$ mode.

Figure 2b shows a series of vertically offset transmission spectra for decreasing cavity length (bottom to top). The two polariton branches and their anticrossing about the exciton energy (gray dashed line) are clearly visible. We note that the cavity could not be closed beyond ≈450 nm, likely due to the size of the bacteria within the cavity.

Figure 2c,d shows the microcavity transmission as the $q = 3$ cavity mode is scanned through the exciton energy. While an anticrossing is again visible, the mode splitting is reduced to 78 meV. This is because of a reduction in the interaction potential due to the weaker EM field within the cavity. For the $q = 4$ mode (Figure 2e,f), the splitting energy is reduced again to 50 meV, and the anticrossing is not clearly resolvable.

The magnitude of the Rabi splitting allows us to put bounds on the number of pigment molecules, and hence the number of bacteria involved in the coupling. We find that the number of excitons simultaneously coupled to the $q = 2$ cavity mode is ≈95 million if all chlorosomes are oriented in the plane of the cavity, and ≈220 million if all dipoles are randomly oriented in the cavity (see the Experimental Section). Assuming 200 000 BChl molecules per chlorosome, the splitting corresponds to the coupling of excitons from between 470 and 1100 chlorosomes, approximately the number that is in 2–6 bacteria.

In order to ascertain whether the bacteria are alive during strong coupling, we have performed microextinction spectroscopy on the bacteria involved in the coupling. A real-space CCD image of the cavity is shown in **Figure 3**a. The cavity was opened to ≈100 µm to allow a continuum of photonic states, and the normalized extinction spectrum of the region marked **1** in Figure 3a is shown in Figure 3b (green line). This is the region from which the transmission spectra in Figure 2 were recorded. We see that there is a strong absorption peak at 750 nm due to the chlorosome absorption, but no sign of TB absorption in the 500–650 nm range, indicating that the cells had not been stained and remained viable. For comparison, the microextinction spectrum of an area containing compromised bacteria is also shown (blue line) where TB absorption is the dominant feature. While the cavity acts to restrict the intensity of light reaching the bacteria, they are known to survive in extremely low light environments and display a low mortality rate even in the presence of no light,[44] making long-term experiments based on bacterial growth rates feasible. Indeed, the bacteria under investigation remained unstained for the duration of the experiment, totaling several hours.

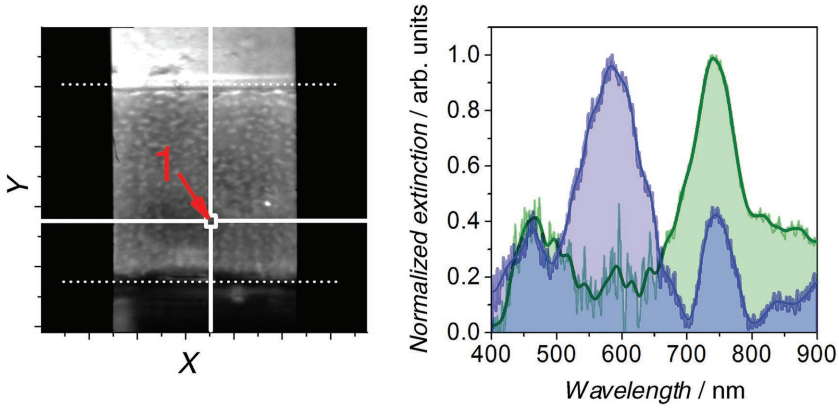

Figure 3. a) Real-space optical image of the microcavity. White dashed lines mark the extent of the plinth in the vertical direction. White solid vertical line represents the position of the spectrometer slit when performing spectral imaging. White solid horizontal line represents the position of the CCD track used for the spectra showing strong coupling shown in Figure 2. The intersection of the solid lines (marked **1**) is the position of the bacteria that are shown to undergo strong coupling to the cavity. The bacteria appear as pale spots on the image, however, they are not clearly individually resolvable as they are smaller than the resolution of the microscope. b) Normalized absorption spectrum taken at position **1** when the cavity was opened to allow a continuum of photonic states (green line), and normalized absorption spectrum of stained bacteria (blue line). In both cases, the absorption spectra were taken from a spectral image, with the reference taken from the same image but a separate track where no bacteria are present.

We have previously suggested that the polariton branches may provide an alternative pathway for excitons to migrate through the photosynthetic system, bypassing various states.[35] The baseplate exciton wavelength is at 790 nm, while the FMO and reaction center are positioned at 810 and 840 nm, respectively. In the current experiment, the polariton branch energy can be widely tuned via the cavity length, and can be brought into energetic resonance with each of these structures as shown in **Figure 4**. For coupling to the $q = 2$ cavity mode, the LPB is resonant with the baseplate at a cavity length of 560 nm, the FMO complex at 580 nm, and the reaction center at 605 nm. The LPB may therefore potentially act as a relaxation pathway for excitons from the chlorosome into lower energy states, including directly into the reaction center, with the final state selectable via the cavity length. The relaxation times associated with exciton transfer through the light harvesting system range from ≈1 to 200 ps,[37,45,46] whereas polaritons in J-aggregate-based microcavity structures have been shown to relax to lower lying exciton states on sub-picosecond timescales.[47] This rapid polariton relaxation may make such a transfer process favorable in comparison to the conventional exciton transfer processes. Indeed, by selectively bypassing subunits of the photosystem, it may be possible to compare the relative efficiencies of each exciton transfer step, perhaps even increasing the efficiency of the photosystem as a whole which could be elucidated directly through observing bacterial growth rates.

Furthermore, there exists the opportunity to create hybrid-polariton systems in which the optical mode that

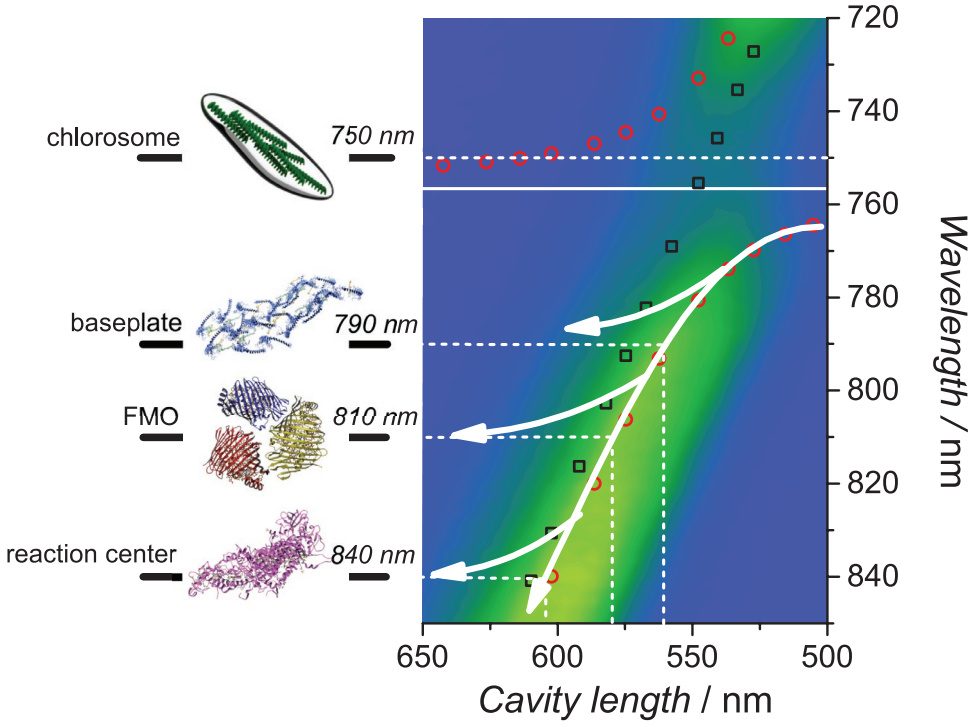

Figure 4. (Left) Energy levels of the components involved in exciton transport in GSB. (Right) Polariton dispersion of bacteria coupled to the $q = 2$ cavity mode, showing possible relaxation pathways that could be accessed by changing the microcavity length.

is coupled to the chlorosome assembly is also coupled to a second semiconductor material placed within the optical cavity. This approach has previously been used to hybridize a range of different semiconductor systems, including different species of molecular dyes,[48] molecular dyes with semiconductor quantum wells,[49,50] and recently molecular dyes with 2D transition metal dichalcogenides (TMDs).[51] By placing GSB in a cavity with a second material that is able to couple to the cavity mode, polariton states may be formed that are simultaneously composed of the chlorosome exciton, the exciton of the second system, and the cavity photon. This mixing of exciton states (optical hybridization) in the strong coupling regime has been shown to facilitate rapid energy transfer between Frenkel-exciton states by virtue of the intermediate hybrid polariton.[52,53] Here, it will be in principle possible to select a second excitonic material having an optical transition that is either lower or higher in energy than that of the chlorosome exciton. This opens an opportunity to either extract or inject energy into the bacteria through control of relative energy levels. The ability to control photosynthesis using such techniques will be of fundamental interest and may allow us to design photosynthetic systems having increased light harvesting efficiency.

In conclusion, we have introduced living photosynthetic bacteria into a photonic microcavity and shown that the system can enter the strong coupling regime, thus creating polariton states within a living organism. This is a demonstration of the noninvasive modification of the innate energy levels within a living system through use of a photonic structure. Such bio-optical engineering could also be used to explore the extent to which photosynthesis can be enhanced in living bacteria by modification of its ability to harvest light. It will also be interesting to explore the extent to which such photonic coupling can be used to modify the function or even direct the growth or survival of an organism whose electronic states are delocalized and shared with its neighbors.

Experimental Section

Calculation of the Cavity Length and Polariton Branch Fitting: In order to calculate the cavity length for each spectrum presented in Figure 2, an area of the spectral image is selected where no strong coupling is observed (i.e., there is no bacteria or too few in a given area to couple). The cavity length L was set such that several Fabry–Perot modes are observed in transmission. The mode index q of each of the modes was calculated from the wavelengths of adjacent modes λ_q and λ_{q-1} using Equation (1):

$$q = \frac{\lambda_{q-1}}{\lambda_{q-1} - \lambda_q} \tag{1}$$

Once the mode index of a transmission peak is known, the cavity length can be calculated via Equation (2):

$$L = \frac{\lambda_q q}{2n} \tag{2}$$

where n is the intracavity refractive index, which we approximate to be that of water, 1.33.

The energy of the lower and upper polariton branches is given by a coupled oscillator model (Equation (3)):[42]

$$\begin{pmatrix} E_c(L) & \hbar\Omega/2 \\ \hbar\Omega/2 & E_x \end{pmatrix} \begin{pmatrix} \alpha_c(L) \\ \alpha_x(L) \end{pmatrix} = E_p(L) \begin{pmatrix} \alpha_c(L) \\ \alpha_x(L) \end{pmatrix} \tag{3}$$

where $E_c(L)$ is the uncoupled cavity mode energy (which is found from Equation (2)), E_x is the exciton energy, $E_p(L)$ is the polariton energy, and $\alpha_c(L)$ and $\alpha_x(L)$ are photon and exciton mixing coefficients, respectively. The polariton branch energies are then given by Equation (4):

$$E_p(L) = \frac{E_c(L) + E_x}{2} \pm \sqrt{\left(E_c(L) - E_x\right)^2 + \hbar\Omega^2} \tag{4}$$

This is fitted to the observed polariton branch energies with $\hbar\Omega$ and n as a fitting parameters. We note that refractive index of the bacteria varies slightly from that of the background index of water,[54] and from the fitting we find that $n = 1.38$, $n = 1.36$, and $n = 1.35$ for the $q = 2$, $q = 3$, and $q = 4$ cavity modes, respectively, commensurate with a larger fraction of the cavity length being occupied by bacteria for smaller cavity lengths leading to a slightly higher value for n. The eigenvalues (mixing coefficients) $\alpha_c(L)$ and $\alpha_x(L)$ are given by Equation (5):

$$\alpha^2_{c,UPB}(L) = \frac{E_c(L) - E_{p,UPB}(L)}{E_x + E_c(L) - 2E_{p,UPB}(L)}, \quad \alpha^2_{x,UPB}(L) = 1 - \alpha^2_{c,UPB}(L)$$
$$\alpha^2_{c,LPB}(L) = \alpha^2_{x,UPB}(L), \quad \alpha^2_{x,LPB}(L) = \alpha^2_{c,UPB}(L) \tag{5}$$

Calculation of the Number of Coupled Dipoles: The Rabi splitting energy $\hbar\Omega$ increases as the square root of the number of dipoles coupled to the field N, with the magnitude of the splitting given by Equation (6):[55]

$$\hbar\Omega = 2\left(\boldsymbol{\mu}.\hat{\boldsymbol{E}}\right)\sqrt{N}\left(\frac{\pi\hbar c}{n_{\text{eff}}^2 \lambda \epsilon_0 V}\right)^{\frac{1}{2}} \tag{6}$$

where $\boldsymbol{\mu}$ is the coupled dipole moment, V is the cavity mode volume, and $\hat{\boldsymbol{E}}$ is a unit vector parallel to the polarization of the cavity electric field. The dipole moment of BChl *c* is 5.48 D,[56] and the cavity mode volume[57] of the $q = 2$ mode is calculated to be $\approx 15\left(\frac{\lambda}{n}\right)^3$. Hence, the number of coupled dipoles can be directly inferred from the Rabi splitting energy if assumptions are made about the relative orientation of the dipoles to the cavity field.

Acknowledgements

D.C. and D.G.L. thank EPSRC Grant No. EP/M025330/1 "Hybrid Polaritonics." D.C., R.A.T., and J.M.S. gratefully acknowledge the Oxford Martin School. L.C.F. acknowledges funding from the Leverhulme Trust. S.K.S. and A.A.G. thank the Center for Excitonics, an Energy Frontier Research Center funded by the U.S. Department of Energy, Office of Science and Office of Basic Energy Sciences, under Award No. DE-SC0001088. S.K.S. also acknowledges the Ministry of Education and Science of the Russian Federation for

supporting the research in the framework of the state assignment, Award No. 3.2166.2017/4.6. V.V. thanks the Oxford Martin School, Wolfson College, and the University of Oxford, the Leverhulme Trust (UK), the John Templeton Foundation, the EU Collaborative Project TherMiQ (Grant Agreement No. 618074), the COST Action MP1209 and the EPSRC (UK). This research was also supported by the National Research Foundation, Prime Minister's Office, Singapore, under its Competitive Research Programme (CRP Award No. NRF- CRP14-2014-02) and administered by Centre for Quantum Technologies, National University of Singapore. D.C. further thanks EPSRC Grant No. EP/K032518/1 "Characterisation of Nanomaterials for Energy."

Conflict of Interest

The authors declare no conflict of interest.

[1] D. H. Hubel, *Eye, Brain and Vision*, 2nd ed., W. H. Freeman, New York **1995**.
[2] B. Ke, *Photosynthesis: Photobiochemistry and Photobiophysics*, Kluwer Academic, Dordrecht, Netherlands **2003**.
[3] O. Shimomura, *Bioluminescence: Chemical Principles and Methods*, World Scientific, Singapore **2012**.
[4] H. A. Frank, R. L. Christensen, *Carotenoids, Vol. 4: Natural Functions*, Birkhäuser Verlag, Basel, Switzerland **2008**.
[5] P. Vukusic, J. R. Sambles, *Nature* **2003**, *424*, 852.
[6] K. J. McGraw, *Bird Coloration, Vol. 1: Mechanisms and Measurements*, Harvard University Press, Cambridge, MA **2006**.
[7] J. W. Galusha, L. R. Richey, J. S. Gardner, J. N. Cha, M. H. Bartl, *Phys. Rev. E* **2008**, *77*, 050904.
[8] L. Biró, J. Vigneron, *Laser Photonics Rev.* **2011**, *5*, 27.
[9] S. Vignolini, E. Moyroud, B. J. Glover, U. Steiner, *J. R. Soc. Interface* **2013**, *10*, 20130394.
[10] S. Kinoshita, *Structural Colors in the Realm of Nature*, World Scientific, Singapore **2008**.
[11] F. Liu, B. Dong, X. Liu, *Optical Devices in Communication and Computation*, InTech, Croatia **2012**, Ch. 6.
[12] B. T. Cunningham, I. D. Block, L. Chan, N. Ganesh, M. Lu, P. C. Mathias, *Selected Topics in Photonic Crystals and Metamaterials*, World Scientific, Singapore **2011**, Ch. 12.
[13] B. Hamza, M. Srungarapu, A. Kadiyala, J. Dawson, L. Hornak, *Biosensors Based on Nanomaterials and Nanodevices*, CRC Press, Boca Raton, FL **2013**, Ch. 8.
[14] M. Humar, S. H. Yun, *Nat. Photonics* **2015**, *9*, 572.
[15] G. Shambat, S.-R. Kothapalli, J. Provine, T. Sarmiento, J. Harris, S. S. Gambhir, J. Vučković, *Nano Lett.* **2013**, *13*, 4999.
[16] M. C. Gather, S. H. Yun, *Nat. Photonics* **2011**, *15*, 406.
[17] T. Byrnes, N. Y. Kim, Y. Yamamoto, *Nat. Phys.* **2014**, *10*, 803.
[18] A. Amo, D. Sanvitto, F. P. Laussy, D. Ballarini, E. del Valle, M. D. Martin, A. Lemaitre, J. Bloch, D. N. Krizhanovskii, M. S. Skolnick, C. Tejedor, L. Vina, *Nature* **2009**, *457*, 291.
[19] C. Schneider, A. Rahimi-Iman, N. Y. Kim, J. Fischer, I. G. Savenko, M. Amthor, M. Lermer, A. Wolf, L. Worschech, V. D. Kulakovskii, I. A. Shelykh, M. Kamp, S. Reitzenstein, A. Forchel, Y. Yamamoto, S. Höfling, *Nature* **2013**, *497*, 348.
[20] J. Kasprzak, M. Richard, S. Kundermann, A. Baas, P. Jeambrun, J. M. J. Keeling, F. M. Marchetti, M. H. Szymanska, R. Andre, J. L. Staehli, V. Savona, P. B. Littlewood, B. Deveaud, L. S. Dang, *Nature* **2006**, *443*, 409.
[21] P. Bhattacharya, T. Frost, S. Deshpande, M. Z. Baten, A. Hazari, A. Das, *Phys. Rev. Lett.* **2014**, *112*, 236802.
[22] J. D. Plumhof, T. Stöferle, L. Mai, U. Scherf, R. F. Mahrt, *Nat. Mater.* **2014**, *13*, 247.
[23] K. S. Daskalakis, S. A. Maier, R. Murray, S. Kéna-Cohen, *Nat. Mater.* **2014**, *13*, 271.
[24] C. Weisbuch, M. Nishioka, A. Ishikawa, Y. Arakawa, *Phys. Rev. Lett.* **1992**, *69*, 3314.
[25] N. Antoine-Vincent, F. Natali, D. Byrne, A. Vasson, P. Disseix, J. Leymarie, M. Leroux, F. Semond, J. Massies, *Phys. Rev. B* **2003**, *68*, 153313.
[26] D. G. Lidzey, D. D. C. Bradley, M. S. Skolnick, T. Virgili, S. Walker, D. M. Whittaker, *Nature* **1998**, *395*, 53.
[27] T. W. Ebbesen, *Acc. Chem. Res.* **2016**, *49*, 2403.
[28] N. Takada, T. Kamata, D. D. C. Bradley, *Appl. Phys. Lett.* **2003**, *82*, 1812.
[29] X. Liu, T. Galfsky, Z. Sun, F. Xia, E.-C. Lin, Y.-H. Lee, S. Kéna-Cohen, V. M. Menon, *Nat. Photonics* **2015**, *9*, 30.
[30] L. C. Flatten, Z. He, D. M. Coles, A. A. P. Trichet, A. W. Powell, R. A. Taylor, J. H. Warner, J. M. Smith, *Sci. Rep.* **2016**, *6*, 33134.
[31] C. P. Dietrich, A. Steude, L. Tropf, M. Schubert, N. M. Kronenberg, K. Ostermann, S. Höfling, M. C. Gather, *Sci. Adv.* **2016**, *2*, 1.
[32] R. M. A. Vergauwe, J. George, T. Chervy, J. A. Hutchison, A. Shalabney, V. Y. Torbeev, T. W. Ebbesen, *J. Phys. Chem. Lett.* **2016**, *7*, 4159.
[33] A. Tsargorodska, M. L. Cartron, C. Vasilev, G. Kodali, O. A. Mass, J. J. Baumberg, P. L. Dutton, C. N. Hunter, P. Törmä, G. J. Leggett, *Nano Lett.* **2016**, *16*, 6850.
[34] D. M. Coles, Y. Yang, Y. Wang, R. T. Grant, R. A. Taylor, S. K. Saikin, A. Aspuru-Guzik, D. G. Lidzey, J. K.-H. Tang, J. M. Smith, *Nat. Commun.* **2014**, *5*, 5561.
[35] S. K. Saikin, Y. Khin, J. Huh, M. Hannout, Y. Wang, F. Zare, A. Aspuru-Guzik, J. K.-H. Tang, *Sci. Rep.* **2014**, *4*, 5057.
[36] J. Overmann, *The Prokaryotes*, 3rd ed., Springer, New York **2006**.
[37] G. S. Orf, R. E. Blankenship, *Photosynth. Res.* **2013**, *116*, 315.
[38] G. Oostergetel, H. Amerongen, E. Boekema, *Photosynth. Res.* **2010**, *104*, 245.
[39] D. Cadena-Herrera, J. E. E.-D. Lara, N. D. Ramirez-Ibanez, C. A. Löpez-Morales, N. O. Pérez, L. F. Flores-Ortiz, E. Medina-Rivero, *Biotechnol. Rep.* **2015**, *7*, 9.
[40] A. V. Kavokin, J. Baumberg, G. Malpuech, F. Laussy, *Microcavities*, Oxford University Press, Oxford **2007**.
[41] A. Fainstein, B. Jusserand, *Light Scattering in Solids IX: Novel Materials and Techniques*, Springer-Verlag, Berlin **2007**, Ch. 6.
[42] M. S. Skolnick, T. A. Fisher, D. M. Whittaker, *Semicond. Sci. Technol.* **1998**, *13*, 645.
[43] D. Bajoni, *J. Phys. D: Appl. Phys.* **2012**, *45*, 313001.
[44] H. V. Gemerden, J. Mas, *Anoxygenic Photosynthetic Bacteria*, Kluwer Academic, Dordrecht, Netherlands **1995**, Ch. 4.
[45] J. Martiskainen, J. Linnanto, V. Aumanen, P. Myllyperki, J. Korppi-Tommola, *Photochem. Photobiol.* **2012**, *88*, 675.
[46] M. Mohseni, P. Rebentrost, S. Lloyd, A. Aspuru-Guzik, *J. Chem. Phys.* **2008**, *129*, 174106.
[47] T. Virgili, D. Coles, A. M. Adawi, C. Clark, P. Michetti, S. K. Rajendran, D. Brida, D. Polli, G. Cerullo, D. G. Lidzey, *Phys. Rev. B* **2011**, *83*, 245309.
[48] D. G. Lidzey, D. D. C. Bradley, A. Armitage, S. Walker, M. S. Skolnick, *Science* **2000**, *288*, 1620.
[49] R. J. Holmes, S. Kéna-Cohen, V. M. Menon, S. R. Forrest, *Phys. Rev. B* **2006**, *74*, 235211.
[50] J. Wenus, R. Parashkov, S. Ceccarelli, A. Brehier, J.-S. Lauret, M. S. Skolnick, E. Deleporte, D. G. Lidzey, *Phys. Rev. B* **2006**, *74*, 235212.
[51] L. C. Flatten, D. M. Coles, Z. He, D. G. Lidzey, R. A. Taylor, J. H. Warner, J. M. Smith, *Nat. Commun.* **2016**, *8*, 14097.
[52] D. M. Coles, N. Somaschi, P. Michetti, C. Clark, P. G. Lagoudakis, P. G. Savvidis, D. G. Lidzey, *Nat. Mater.* **2014**, *13*, 712.

[53] X. Zhong, T. Chervy, S. Wang, J. George, A. Thomas, J. A. Hutchison, E. Devaux, C. Genet, T. W. Ebbesen, *Angew. Chem., Int. Ed.* **2016**, *55*, 6202.
[54] P. Liu, L. Chin, W. Ser, T. Ayi, P. Yap, T. Bourouina, Y. Leprince-Wang, *Proc. Eng.* **2014**, *87*, 356.
[55] M. Fox, *Quantum Optics: An Introduction*, Oxford University Press, Oxford **2006**, Ch. 10.
[56] V. Prokhorenko, D. Steensgaard, A. Holzwarth, *Biophys. J.* **2000**, *79*, 2105.
[57] K. Ujihara, *Jpn. J. Appl. Phys.* **1991**, *30*, L901.

Received: May 28, 2017
Revised: July 8, 2017
Published online: August 15, 2017

